Cendana International Conference on Social and Technology (CICoST)
1st CISoST - 2023
E-ISSN: 3047-2490
August 2023
Page: 130 - 138

Segmentation of Skin Cancer Images Using Fully Convolutional DenseNet - Tiramisu (One Hundred Layers)

Primatua Sitompul[1*], Rika Rosnelly[2], Wanayumini[3]

[1,2,3] Universitas Potensi Utama, Medan, Indonesia
Email: [1*]prima.sitompul@gmail.com, [2]rikarosnelly@gmail.com, [2]wanayumini@gmail.com
(* : coressponding author)

Abstrak

The success of identification of skin cancer images based on Computer Aided System (CAD) cannot be separated from the results of segmentation of skin lesions. The segmentation of cancer images automatically becomes a challenge because of the large variety of skin colors, irregular shapes, and the boundary between the skin and the lesion that is at least clear or irregular. The presence of artifacts such as hair, bubbles, rulers, and black blocks contained in the dermoscopy image is very disturbing and requires additional methods to perform a skin recognition system. In this study, an experimental segmentation of the skin lesion area on skin cancer dermoscopy images was carried out using three Fully Convolutional DenseNet – Tiramisu (One Hundred Layers) architectural models, namely FC-DenseNet 103, FC-DenseNet 67, and FC-DenseNet 56 against the HAM10000 dataset. From the third model used, testing with 100 epochs against FC-DenseNet 103 got the highest results from the other models. The evaluation was carried out with the metric parameter Intersection of Union (IoU architecture FC-DenseNet 103, FC-DenseNet 67 and FC-DenseNet 56 respectively got a value of 83.85%, an accuracy of 81.85% and 76.77%. Meanwhile, evaluation using the Dice Coefficient metric parameter, FC-DenseNet 103, FC-DenseNet 67 and FC-DenseNet 56 architectures, respectively, get values of 91.09%, 89.88%, 88.59%. From the test results, it is known that the number of layers in the FC-DenseNet - Tiramisu model affects the segmentation results.

Keyword: Skin Cancer, Segmentation, CNN, FC-DenseNet, Tiramisu

1. INTRODUCTION

Automated skin cancer identification based on Computer Vision is a challenging and difficult topic to tackle. This is due to the numerous types of skin cancer, the variation in lesion colors, skin tones, and the imbalance in available datasets. Other difficulties and challenges include variations in brightness, lighting conditions, the presence of artifacts (Alom et al., 2019), such as hair, air bubbles, and significant variability that affects segmentation accuracy (Khan, Sharif, et al., 2021; Phan et al., 2021). Skin cancer is one of the most serious diseases. Every year, the number of patients diagnosed with skin cancer and the number of deaths from this disease increase worldwide. It is estimated that 2-3 million people are diagnosed with non-melanoma skin cancer and 132,000 people with melanoma skin cancer annually (Le et al., 2022)(Khan, Sharif, et al., 2021). According to WHO, the increase in skin cancer patients is due to the rise in ultraviolet radiation caused by the thinning ozone layer in the atmosphere. Other research indicates that besides the influence of ultraviolet radiation, skin cancer can also be affected by genetic factors, unhealthy lifestyles, and human papillomavirus infection (WHO, 2017).

There are many types of skin cancer, but the most common ones are basal cell carcinoma, squamous cell carcinoma, and malignant melanoma (Farooq et al., 2016; Khan, Akram, et al., 2021). Melanoma is the most aggressive, metastatic, and dangerous type of skin cancer (Gurung & Gao, 2020). 75% of skin cancer deaths are caused by melanoma (Hosny et al., 2019). Early diagnosis of skin cancer is necessary (Esteva et al., 2017; Romero Lopez et al., 2017; Talavera-Martinez et al., 2021; Ünver & Ayan, 2019; Vesal et al., 2018) to ensure proper treatment and to prevent the infected cancer cells from spreading to other parts of the body (Thanh et al., 2021). Studies indicate that the survival rate of melanoma patients can reach 90-95% if early detection diagnosis is performed (Hosny et al., 2019; Vesal et al., 2018).

A skin lesion is an area of the skin that has been damaged. The abnormal growth of skin tissue or an appearance different from the surrounding skin can be seen from the skin lesion's appearance. Generally, the diagnosis of indicative skin lesions is based on morphological characteristics, such as irregular shape, asymmetry, varied colors, accompanied by a history of changes in size, shape, color, or texture. These skin lesions are marked by skin pigment darker than the skin's color. Sometimes, skin lesions are not accompanied by pain for the sufferer (Phan et al., 2021). Manual examination of skin lesions is done by first taking dermoscopic images to see the visual details of the skin lesions more clearly. By using dermoscopic imaging techniques, the obtained skin lesion images can be more detailed, and the skin surface reflections during imaging can be eliminated. With this method, dermoscopy experts can study skin lesions better than diagnoses made with the naked eye (Ünver & Ayan, 2019). Manual observation depends heavily on expertise and experience, is time-consuming (Anjum et al., 2020), prone to errors (Al-masni et al., 2018), and subjective and inconsistent (Phan et al., 2021). Therefore, Computer-Aided Diagnosis (CAD) systems have been developed to help speed up the diagnosis process (Talavera-Martinez et al., 2021). Automatic skin cancer diagnosis with CAD systems uses dermoscopic images as input. The identification and classification of the disease with this system generally use image preprocessing, segmentation, feature extraction, and classification (Ünver & Ayan, 2019). In the skin

E-ISSN: 3047-2490
August 2023
Page: 130 - 138

lesion image segmentation process, the results provide information about the skin lesion, such as border, shape, asymmetry, and irregularity (Anjum et al., 2020). The main challenge in segmenting skin lesions is the diversity in color, shape, texture, size, irregular shapes, and unclear borders of the skin lesions (Al-masni et al., 2018). Additionally, the presence of blood vessels, hair, and low contrast between skin tissues (Tang et al., 2019). Manual segmentation of skin cancer images is time-consuming (Bi et al., 2017), and inaccurate (Yang et al., 2021), especially when segmentation must be performed on a large and diverse number of images.

In this research, dermoscopic image segmentation is carried out using the Fully Convolution DenseNet (FC-DenseNet) – Tiramisu (One Hundred Layers) architecture. Tiramisu is one of the DenseNet architecture networks, consisting of dense blocks and pooling layers. DenseNet is more efficient in parameter usage, has short paths on feature maps similar to Deeply Supervised Networks, and all layers can easily access previous layers to reuse information from previously calculated feature maps (Simon et al., 2017). This method was chosen because the segmentation results obtained with the Tiramisu architecture were better than the U-Net architecture in Sclerosis lesion segmentation (Zhang et al., 2019). In the Tiramisu model, upsampling and downsampling paths are added, similar to decoders and encoders, to recover input resolution. Tiramisu, even with very few parameters, achieves better global accuracy for semantic segmentation on the CamVid dataset compared to other models like SegNet, Bayesian SegNet, DeconvNet, DeepLab-LFOV, and Dilation8 + FSO (Simon et al., 2017).

2. RESEARCH METHODE

2.1 Research Framework

To perform automatic segmentation on dermoscopic images using the FC-DenseNet Tiramisu method, this study includes several stages: data collection, hair removal, training data to obtain segmentation results, and testing and evaluating the segmentation results with the Tiramisu architecture.

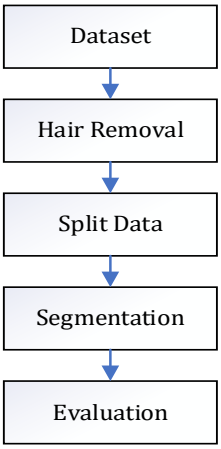

Figure 1. Block diagram of research

In this study, the process of dermoscopic image segmentation was conducted using Jupyter Notebook, Anaconda Python 3.9, and TensorFlow 2.7 on a notebook device with the specifications of an AMD Ryzen 7 processor, 2.9 GHz, 8GB RAM, and an NVIDIA GTX 1660Ti GPU.

2.2 Dataset

The dataset used in this study comes from the Human Against Machine (HAM10000) dataset (Tschandl, 2018). The dataset is openly available and can be downloaded from the site https://dataverse.harvard.edu/dataset.xhtml?persistentId=doi:10.7910/DVN/DBW86T with a total size of 2.6 GB. The dataset contains seven types of skin cancer with a total of 10,015 images in ".jpg" format, each sized 600×450 pixels. Dermoscopic images are used by dermatologists in the process of manually inspecting skin lesions or identifying skin cancer using CAD systems. Dermoscopic images are photographs taken during the dermoscopy stage when skin lesion inspection is performed. Dermoscopy is a procedure used to visualize the desired skin area with specific magnification techniques and eliminate surface reflection during image capture (Rahman et al., 2021). The distribution of images in the dataset can be seen in Table 1.

Table 1. Image Distribution in Dataset

Code	Lesion Type	Number of Images
akiec	Actinic keratoses and intraepithelial carcinoma	327
bcc	Basal cell carcinoma	514

E-ISSN: 3047-2490
August 2023
Page: 130 - 138

Code	Lesion Type	Number of Images
bkl	Benign keratosis-like lesions	1.099
bf	Dermatofibroma	115
mel	Melanoma	1.113
nv	Melanocytic nevi	6.705
vasc	vascular lesions	142

In addition to dermoscopic images, the dataset also contains ground truth images. Ground truth represents the areas of the images that indicate skin regions affected by skin cancer based on expert analysis (dermatologists). These ground truth images will subsequently be used as the reference for accuracy during the evaluation phase. Sample dermoscopic images from the dataset can be seen in Figure 2.

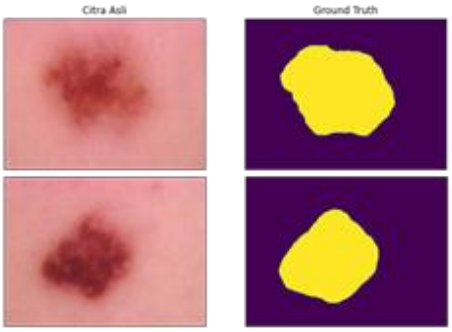

Figure 2. Image Samples in Dataset

2.3 Hair Removal

The presence of hair artifacts in dermoscopic images obscures significant patterns and can reduce the accuracy of the segmentation process. Hair removal is an important and frequently performed method in the image preprocessing stage before data training. Once the hair is detected and removed, the next step is to restore important information such as color and texture patterns. This method is capable of retaining essential information in each pixel of the dermoscopic images (Talavera-Martinez et al., 2021).

Figure 3. Hair Removal Results on Dermoscopic Images

2.4 Data Split

After the hair removal process is completed, the dataset is split with a ratio of 90% for training data and 10% for testing data. From the training data, 20% is taken as validation data during the training process. Then, the image size is reduced to 64×64 pixels to manage the computational load, training time, and memory availability of the device used. The distribution of training, validation, and testing data is shown in Table 2.

Table 2. Training Data Distribution, Validation and Testing

Split Data	Dermoscopy Image	Ground Truth (Mask)
Training Data	7.210	7.210
Validation Data	1.803	1.803
Testing Data	1.002	1.002
Total	**10.015**	**10.015**

2.5 Segmentation

Segmentation is a fundamental stage in the process of identifying or classifying skin cancer images (Phan et al., 2021). Skin lesion segmentation provides crucial information about the lesions, such as borders, shape, asymmetry, and irregularity (Anjum et al., 2020). Segmentation is a quantitative classification process in digital

E-ISSN: 3047-2490
August 2023
Page: 130 - 138

image processing that can also be defined as the process of grouping pixels into predefined classes based on the variables used (Wanayumini et al., 2018). The main goal of the segmentation process is to separate the object from the background in an image (Debasu Mengistu & Melesew Alemayehu, 2015), so that feature extraction and identification in subsequent processes can be performed. The efficiency of the segmentation stage affects the accuracy of skin cancer classification (Tang et al., 2019). The segmentation process in this study was conducted by experimenting with three models of Fully Convolutional DenseNet (FC-DenseNet) – Tiramisu (One Hundred Layers) architectures, namely FC-DenseNet 103, FC-DenseNet 67, and FC-DenseNet 56.

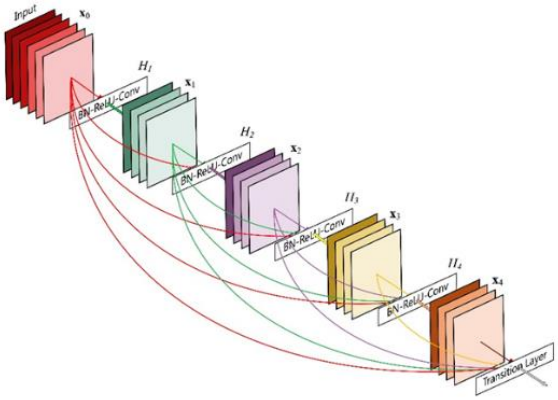

Figure 4. DenseNet Network

2.6 Fully Convolutional DenseNet (FC-DenseNet) -Tiramisu (One Hundred Layer)

Densely Connected Convolutional Networks (DenseNet) are a type of Convolutional Neural Network (CNN) architecture known for their effective performance in image classification. In DenseNet, each layer is connected to every subsequent layer. At each layer, the feature maps from all preceding layers are treated as separate inputs, while its own feature map is passed as input to all subsequent layers. The building blocks of DenseNet consist of densely connected blocks that utilize skip connections between layers to facilitate information flow and gradients. Fully Convolutional Networks (FCNs) were introduced as an extension of CNNs to address pixel-wise prediction tasks in semantic segmentation. In FCNs, upsampling layers are added to standard CNN architectures to recover spatial input resolution in the output layers. FC-DenseNet networks combine downsampling paths, upsampling paths, and skip connections. Skip connections assist the upsampling path in recovering detailed spatial information from the downsampling path using feature maps. Consequently, FCNs can process images of varying sizes. To compensate for the loss of resolution caused by pooling layers, FCNs establish connections between downsampling and upsampling paths (Simon et al., 2017)

The training and testing processes in the Tiramisu network are similar to the U-Net architecture (Singh & Das, 2020), which includes downsampling, bottleneck, upsampling paths, and skip connections. In Tiramisu, there are downsampling and upsampling paths similar to a decoder structure. Tiramisu extends the use of DenseNet to function like FCNs by adding an upsampling path to fully restore input resolution. Constructing a natural upsampling path would result in a large number of feature maps that are computationally challenging with very high resolutions before the softmax layer. Therefore, Tiramisu samples from the feature maps generated by the preceding dense blocks to mitigate this effect. This approach allows for a consistent number of dense blocks at each resolution in the upsampling path, independent of the number of pooling layers. Additionally, upsampled dense blocks combine information from other dense blocks at the same resolution via skip connections between the downsampling and upsampling paths (Simon et al., 2017). The architectural structure of Tiramisu can be visualized as depicted in Figure 5.

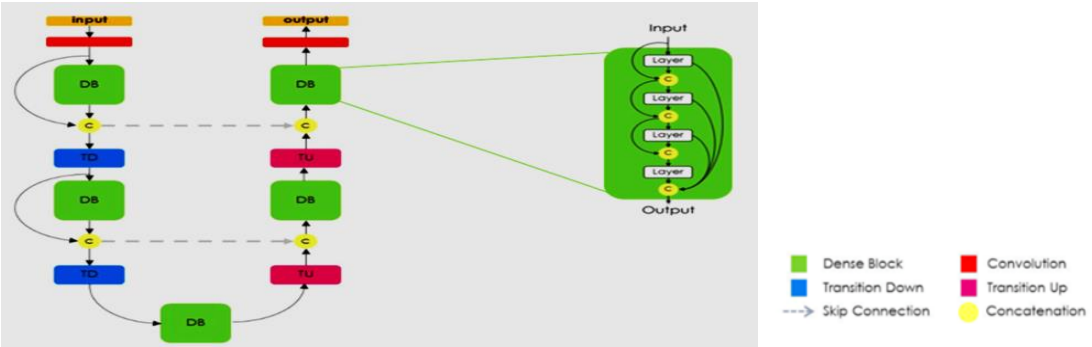

Figure 5. Tiramisu Network Architecture - One Hundred Layers

E-ISSN: 3047-2490
August 2023
Page: 130 - 138

Broadly speaking, there are three main components in the Tiramisu model: Dense Block, Transition Up, and Transition Down. The first layer after the input and the last layer before the output are convolution layers. The output from the convolution layer is then passed to the Dense Block (DB), followed by a concatenation operation. Each Dense Block consists of multiple layers and repeated concatenation computations. This process is then repeated in the subsequent stages until the final layer. Each value produced in the previous process is passed to the next process. The difference lies in the computation processes in the Transition Down and Transition Up stages. For more details on the layers in each Dense Block, Transition Up, and Transition Down, refer to Table 3.

Table 3. Layer Composition in Dense Block, Transition Down and Transition Up

Layer	Transition Down	Transition Up
Batch Normalization	Batch Normalization	3x3 Tranposed Convolution
ReLU	ReLU	Stride = 2
3x3 Convolution	1x1 Convolution	
Dropout p=0.2	Dropout p=0.2	
	2x2 Max pooling	

Each layer within the Dense Block includes batch normalization, ReLU activation, a 3×3 convolution layer, and Dropout with a dropout rate p = 0.2, In the Transition Down stage, there is batch normalization, ReLU activation, a 3×3 convolution layer, Dropout with a dropout rate p = 0.2, and Max Pooling 2×2. On the other hand, in the Transition Up stage, there is Transposed Convolution with a stride of 2.

2.7 Evaluation Metrics

Metric evaluation plays an important role in assessing segmentation results (Jadon, 2020). Jaccard index and Dice Score are the most popular methods for evaluating matrix performance in image segmentation (Bertels et al., 2019).

2.7.1 Intersection Of Union (IoU) / Jaccard Index

The Jaccard Index, also known as the Jaccard Similarity Coefficient or Intersection over Union (IoU), is a method commonly used to evaluate the similarity between two sets of samples. Its purpose is to compare predictions from training against ground truth (Shamir et al., 2018). During this stage, the Jaccard Index determines the ratio of intersection or overlap between detected objects in the training set and measures its correlation with the ground truth (Ünver & Ayan, 2019). The Jaccard Index evaluates the prediction obtained from segmentation and computes the intersection with the ground truth. The result is then divided by the union of the prediction segmentation and ground truth. The process of Jaccard Similarity can be visualized in Figure 6.

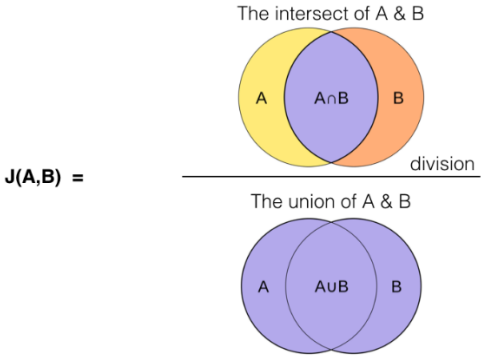

Figure 6. Intersection Of Union (IoU)

The *IoU* metric provides a value in the range of 0 (if there is no similarity between the pixels in the G_I and S_I) to 1 (if the pixels between the G_I and S_I match very well). The Jaccard Similarity equation is as follows:

$$J(A,B) = \frac{|A \cap B|}{|A \cup B|} = \frac{|A \cap B|}{|A|+|B|-|A \cap B|} \quad (1)$$

If the segmentation prediction in image I is S_I and the ground truth in image I is G_I, then the equation can be written as follows:

$$IoU(I) = \frac{S_I \cap G_I}{S_I \cup G_I} \quad (2)$$

2.7.2 Dice Similarity Coefficient

Dice Score was first introduced to evaluate the results of automatic lesion segmentation (Bertels et al., 2019). Dice similarity coefficient or also called the Sørensen–Dice index, is an instrument commonly used to measure

E-ISSN: 3047-2490
August 2023
Page: 130 - 138

the similarity between two data sets (Jadon, 2020). Dice coefficient is used as an indicator to evaluate segmentation results (Yang et al., 2021)(Goyal et al., 2020) against ground truth. The dice coefficient equation can be seen in equation (3).

$$\frac{2*|X \cap Y|}{(|X|+|Y|)} \quad (3)$$

2.8 Hyperparameter

Hyperparameters are variables used during the training process. The hyperparameters used in the model in this study include learning rate, batch size, epoch, activation function, drop out, max pooling and stride.

3. RESULT AND DISCUSSION

To evaluate the performance of the three Tiramisu architecture models – FC-DenseNet 103, FC-DenseNet 67, and FC-DenseNet 56 – in segmenting dermoscopy images, hyperparameter adjustments were made. Each model was configured with 100 epochs and a batch size of 20 per epoch. Early stopping and learning rate reduction features were implemented to halt training if no improvement was observed for 10 consecutive epochs. The Dense Block configurations differed among the models, as detailed in Table 4, specifying the number of layers within each Dense Block for FC-DenseNet 103, FC-DenseNet 67, and FC-DenseNet 56.

Table 4. FC-DenseNet 103, FC-DenseNet 67 and FC-DenseNet 56 Architectures

FC-Densenet 103 Architectures	FC-Densenet 67 Architectures	FC-Densenet 56 Architectures
k=16	k=12	k=12
Input, m=3	Input, m=3	Input, m=3
3 × 3 Convolution, m = 48	3 × 3 Convolution, m = 48	3 × 3 Convolution, m = 48
DB (4 layers) + TD, m = 112	DB (4 layers) + TD, m = 96	DB (4 layers) + TD, m = 96
DB (5 layers) + TD, m = 192	DB (4 layers) + TD, m = 144	DB (4 layers) + TD, m = 144
DB (7 layers) + TD, m = 304	DB (4 layers) + TD, m = 192	DB (4 layers) + TD, m = 192
DB (10 layers) + TD, m = 464	DB (4 layers) + TD, m = 240	DB (4 layers) + TD, m = 240
DB (12 layers) + TD, m = 656	DB (4 layers) + TD, m = 288	DB (4 layers) + TD, m = 288
Dense Block (15 layers), m = 896	Dense Block (4 layers), m = 336	Dense Block (4 layers), m = 336
TU + DB (12 layers), m = 1088	TU + DB (4 layers), m = 384	TU + DB (4 layers), m = 384
TU + DB (10 layers), m = 816	TU + DB (4 layers), m = 368	TU + DB (4 layers), m = 368
TU + DB (7 layers), m = 576	TU + DB (4 layers), m = 320	TU + DB (4 layers), m = 320
TU + DB (5 layers), m = 384	TU + DB (4 layers), m = 272	TU + DB (4 layers), m = 272
TU + DB (4 layers), m = 256	TU + DB (4 layers), m = 242	TU + DB (4 layers), m = 242
1 × 1 Convolution, m = c	1 × 1 Convolution, m = c	1 × 1 Convolution, m = c
Softmax	Softmax	Softmax
Total Parameters = 13,818,793	**Total Parameters = 4,923,769**	**Total Parameters = 2,447,137**

TU is the transition up, m is the number of feature maps, TD is the transition down, c is the number of classifications, DB is the dense block, and k is the growth rate layer. Based on the results of experiments and evaluations on the FC-DenseNet 103 architecture, a training accuracy value of 93.23%, IoU of 76.77% and dice coefficient of 88.59% were obtained. The FC-DenseNet 103 architecture takes an average of 77 seconds for each epoch. On the FC-DenseNet 67 architecture, the training accuracy obtained was 93.90%, the IoU value was 81.85%, and the dice coefficient was 89.89%. The FC-DenseNet 67 architecture takes an average of 104 seconds for each epoch. Experiments on the FC-DenseNet 103 architectural model, obtained an accuracy value of 94.14%, an IoU of 82.58%, and a dice coefficient of 90.35%. With an average time required of 120 seconds for each epoch.

Table 5. Tiramisu Architecture Training Results

Architectures	Acc	IoU	Dice Coef	Time
FC-DenseNet 56	93.23	76.77	88.59	77 detik
FC-DenseNet 67	93.90	81.85	89.88	105 detik
FC-DenseNet 103	94.14	83.85	91.09	120 detik

Based on the three models tested, FC-Densenet 103 is superior in segmenting dermoscopic images, but with compensation for a longer training time compared to other architectures. From the table it can be seen that FC-Densenet 56, which has a total number of parameters of 2,447,137, obtained quite good accuracy, namely with an accuracy value of 93.23% with a more efficient training time compared to the other two models. Based on

E-ISSN: 3047-2490
August 2023
Page: 130 - 138

observations of the segmentation results, a comparison can be seen between ground truth and predictions in the dermoscopic image segmentation produced by the tiramisu model as shown in Figure 7.

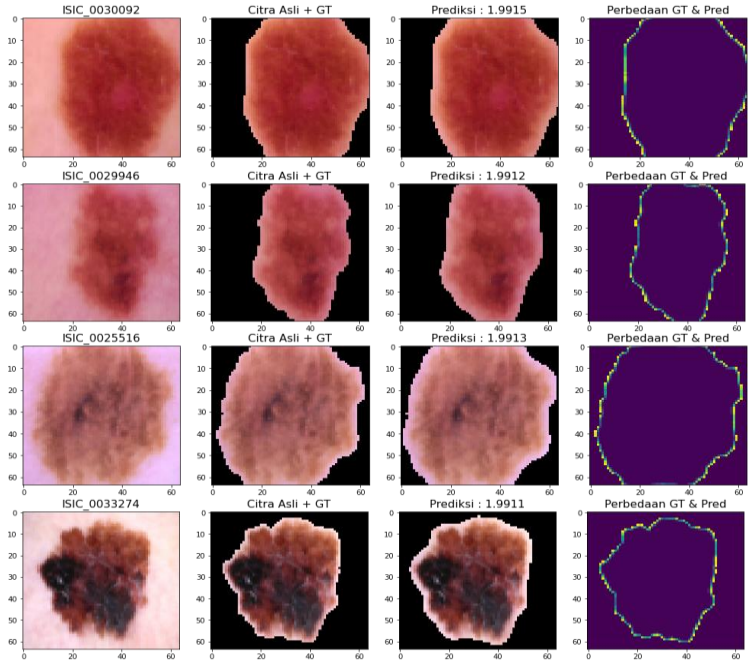

Figure 7. Segmentation prediction results

Segmentation prediction failure was found in skin lesion areas that did not have a clear border or the contrast between the lesion and the skin was very faint. Analysis of the highest error value obtained, the model was unable to detect skin lesion areas in the image *ISIC_0024337.jpg* with the type of basal kertosis.

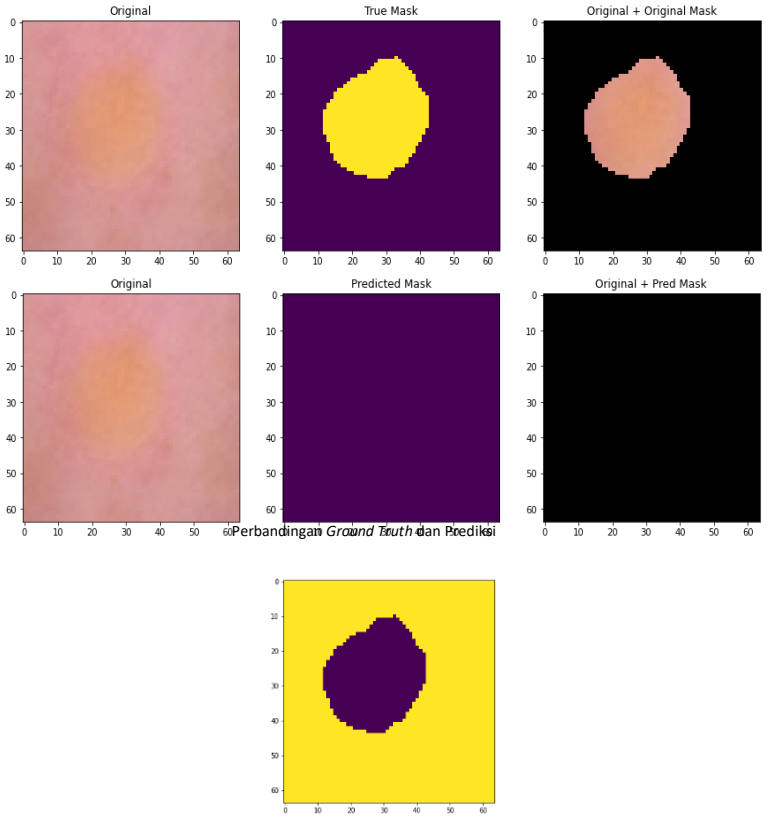

Figure 8. Prediction with the highest error

In Figure 8 it can be seen that the model failed to estimate the indicated skin lesion area. Visually it can be seen that the border or edge between the lesion and the skin color is not clearly visible.

E-ISSN: **3047-2490**
August 2023
Page: **130 - 138**

4. CONCLUSION

Based on the segmentation prediction results of dermoscopy images from the HAM10000 dataset using the Tiramisu architecture, it was found that the FC-DenseNet 103 model performed better compared to the other two models. Evaluation of the segmentation results using the Intersection over Union (IoU) metric showed that FC-DenseNet 103, FC-DenseNet 67, and FC-DenseNet 56 achieved IoU values of 83.85%, 81.85%, and 76.77%, respectively. Meanwhile, evaluation based on the Dice coefficient metric showed that FC-DenseNet 103, FC-DenseNet 67, and FC-DenseNet 56 achieved Dice coefficients of 91.09%, 89.88%, and 88.59%, respectively. These results indicate that FC-DenseNet Tiramisu is highly effective in segmenting skin cancer images. Based on the evaluation results conducted on dermoscopy image samples, it strengthens the conclusion that the contrast between skin color and the color of the lesion area is a critical factor in automatic segmentation or identification of skin cancer. Failures in prediction or prediction errors occur in images with very low contrast between skin color and lesion color, making it difficult for the model to recognize suspected lesion areas. In future research, image pre-processing to enhance the border or contrast between skin and lesions becomes crucial. Pre-processing should be performed prior to segmentation to ensure that the model used in the training process can recognize image areas more effectively.

REFERENCES

Al-masni, M. A., Al-antari, M. A., Choi, M. T., Han, S. M., & Kim, T. S. (2018). Skin lesion segmentation in dermoscopy images via deep full resolution convolutional networks. *Computer Methods and Programs in Biomedicine*, *162*, 221–231. https://doi.org/10.1016/j.cmpb.2018.05.027

Alom, M. Z., Aspiras, T., Taha, T. M., & Asari, V. K. (2019). *Skin Cancer Segmentation and Classification with NABLA-N and Inception Recurrent Residual Convolutional Networks*.

Anjum, M. A., Amin, J., Sharif, M., Khan, H. U., Malik, M. S. A., & Kadry, S. (2020). Deep Semantic Segmentation and Multi-Class Skin Lesion Classification Based on Convolutional Neural Network. *IEEE Access*, *8*, 129668–129678. https://doi.org/10.1109/ACCESS.2020.3009276

Bertels, J., Eelbode, T., Berman, M., Vandermeulen, D., Maes, F., Bisschops, R., & Blaschko, M. B. (2019). Optimizing the Dice Score and Jaccard Index for Medical Image Segmentation: Theory and Practice. *Lecture Notes in Computer Science (Including Subseries Lecture Notes in Artificial Intelligence and Lecture Notes in Bioinformatics)*, *11765 LNCS*, 92–100. https://doi.org/10.1007/978-3-030-32245-8_11

Bi, L., Kim, J., Ahn, E., Kumar, A., Fulham, M., & Feng, D. (2017). Dermoscopic Image Segmentation via Multistage Fully Convolutional Networks. *IEEE Transactions on Biomedical Engineering*, *64*(9), 2065–2074. https://doi.org/10.1109/TBME.2017.2712771

Debasu Mengistu, A., & Melesew Alemayehu, D. (2015). Computer Vision for Skin Cancer Diagnosis and Recognition using RBF and SOM. *International Journal of Image Processing (IJIP)*, *9*(6), 311–319.

Esteva, A., Kuprel, B., Novoa, R. A., Ko, J., Swetter, S. M., Blau, H. M., & Thrun, S. (2017). Dermatologist-level classification of skin cancer with deep neural networks. *Nature*, *542*(7639), 115–118. https://doi.org/10.1038/nature21056

Farooq, M. A., Azhar, M. A. M., & Raza, R. H. (2016). Automatic Lesion Detection System (ALDS) for Skin Cancer Classification Using SVM and Neural Classifiers. *Proceedings - 2016 IEEE 16th International Conference on Bioinformatics and Bioengineering, BIBE 2016*, 301–308. https://doi.org/10.1109/BIBE.2016.53

Goyal, M., Yap, M. H., & Hassanpour, S. (2020). Multi-class semantic segmentation of skin lesions via fully convolutional networks. *BIOINFORMATICS 2020 - 11th International Conference on Bioinformatics Models, Methods and Algorithms, Proceedings; Part of 13th International Joint Conference on Biomedical Engineering Systems and Technologies, BIOSTEC 2020*, 290–294. https://doi.org/10.5220/0009380302900295

Gurung, S., & Gao, Y. R. (2020). Classification of melanoma (skin cancer) using convolutional neural network. *CITISIA 2020 - IEEE Conference on Innovative Technologies in Intelligent Systems and Industrial Applications, Proceedings*, *10*(3), 1–8. https://doi.org/10.1109/CITISIA50690.2020.9371829

Hosny, K. M., Kassem, M. A., & Foaud, M. M. (2019). Classification of skin lesions using transfer learning and augmentation with Alex-net. *PLoS ONE*, *14*(5), 1–17. https://doi.org/10.1371/journal.pone.0217293

Jadon, S. (2020). A survey of loss functions for semantic segmentation. *2020 IEEE Conference on Computational Intelligence in Bioinformatics and Computational Biology, CIBCB 2020*. https://doi.org/10.1109/CIBCB48159.2020.9277638

Khan, M. A., Akram, T., Sharif, M., Kadry, S., & Nam, Y. (2021). Computer Decision Support System for Skin Cancer Localization and Classification. *Computers, Materials and Continua*, *68*(1), 1041–1064. https://doi.org/10.32604/cmc.2021.016307

Khan, M. A., Sharif, M., Akram, T., Damaševičius, R., & Maskeliūnas, R. (2021). Skin lesion segmentation and multiclass classification using deep learning features and improved moth flame optimization. *Diagnostics*, *11*(5). https://doi.org/10.3390/diagnostics11050811

Le, D. N. T., Le, H. X., Ngo, L. T., & Ngo, H. T. (2022). Transfer learning with class-weighted and focal loss function for automatic skin cancer classification. In *arXiv:2009.05977* (pp. 1–7). https://doi.org/10.48550/arXiv.2009.05977

Phan, T. D. T., Kim, S. H., Yang, H. J., & Lee, G. S. (2021). Skin lesion segmentation by u-net with adaptive skip connection and structural awareness. *Applied Sciences (Switzerland)*, *11*(10). https://doi.org/10.3390/app11104528

Rahman, Z., Hossain, S., Islam, R., & Hasan, M. (2021). Informatics in Medicine Unlocked An approach for multiclass skin lesion classification based on ensemble learning. *Informatics in Medicine Unlocked*, *25*, 100659. https://doi.org/10.1016/j.imu.2021.100659

Romero Lopez, A., Giro-I-Nieto, X., Burdick, J., & Marques, O. (2017). Skin lesion classification from dermoscopic images using deep learning techniques. *Proceedings of the 13th IASTED International Conference on Biomedical Engineering, BioMed 2017*, 49–54. https://doi.org/10.2316/P.2017.852-053

Shamir, R. R., Duchin, Y., Kim, J., Sapiro, G., & Harel, N. (2018). *Continuous Dice Coefficient: a Method for Evaluating Probabilistic Segmentations*. *1*, 1–34. https://doi.org/http://dx.doi.org/10.1101/306977

Simon, J., Drozdzal, M., Vazquez, D., Romero, A., & Bengio, Y. (2017). The One Hundred Layers Tiramisu : Fully Convolutional DenseNets for Semantic Segmentation. *IEEE Conference on Computer Vision and Pattern Recognition Workshops (CVPRW)*, 1175–1183. https://doi.org/10.1109/CVPRW.2017.156

Singh, S., & Das, A. (2020). Study of Brain Region Segmentation Using Convolutional Neural Network. *International Journal on Orange Technologies*, *2*(10), 66–78. https://doi.org/10.31149/ijot.v2i2.711

E-ISSN: **3047-2490**
August 2023
Page: **130 - 138**

Talavera-Martinez, L., Bibiloni, P., & Gonzalez-Hidalgo, M. (2021). Hair Segmentation and Removal in Dermoscopic Images Using Deep Learning. *IEEE Access*, *9*, 2694–2704. https://doi.org/10.1109/ACCESS.2020.3047258

Tang, P., Liang, Q., Yan, X., Xiang, S., Sun, W., Zhang, D., & Coppola, G. (2019). Efficient skin lesion segmentation using separable-Unet with stochastic weight averaging. *Computer Methods and Programs in Biomedicine*, *178*, 289–301. https://doi.org/10.1016/j.cmpb.2019.07.005

Thanh, D. N. H., Hai, N. H., Hieu, L. M., Tiwari, P., & Surya Prasath, V. B. (2021). Skin lesion segmentation method for dermoscopic images with convolutional neural networks and semantic segmentation. *Computer Optics*, *45*(1), 122–129. https://doi.org/10.18287/2412-6179-CO-748

Tschandl, P. (2018). *The HAM10000 dataset, a large collection of multi-source dermatoscopic images of common pigmented skin lesions* (V. Group (ed.); V3 ed.). Harvard Dataverse. https://doi.org/doi/10.7910/DVN/DBW86T

Ünver, H. M., & Ayan, E. (2019). Skin lesion segmentation in dermoscopic images with combination of yolo and grabcut algorithm. *Diagnostics*, *9*(3). https://doi.org/10.3390/diagnostics9030072

Vesal, S., Malakarjun Patil, S., Ravikumar, N., & Maier, A. K. (2018). A multi-task framework for skin lesion detection and segmentation. *Lecture Notes in Computer Science (Including Subseries Lecture Notes in Artificial Intelligence and Lecture Notes in Bioinformatics)*, *11041 LNCS*(September), 285–293. https://doi.org/10.1007/978-3-030-01201-4_31

Wanayumini, W., S Sitompul, O., Zarlis, M., Suwilo, S., & M H Pardede, A. (2018). A Research Framework for Supervised Image Classification For Tornado Chaos Phenomena. *International Journal of Engineering & Technology*, *7*(4.15), 447. https://doi.org/10.14419/ijet.v7i4.15.25254

WHO. (2017). *Radiation: Ultraviolet (UV) radiation and skin cancer*.

Yang, C. H., Ren, J. H., Huang, H. C., Chuang, L. Y., & Chang, P. Y. (2021). Deep Hybrid Convolutional Neural Network for Segmentation of Melanoma Skin Lesion. *Computational Intelligence and Neuroscience*, *2021*. https://doi.org/10.1155/2021/9409508

Zhang, H., Valcarcel, A. M., Bakshi, R., Chu, R., Bagnato, F., Shinohara, R. T., Hett, K., & Oguz, I. (2019). Multiple Sclerosis Lesion Segmentation with Tiramisu and 2.5D Stacked Slices. *Lecture Notes in Computer Science (Including Subseries Lecture Notes in Artificial Intelligence and Lecture Notes in Bioinformatics)*, *11766 LNCS*, 338–346. https://doi.org/10.1007/978-3-030-32248-9_38